



# Novel axially substituted lanthanum phthalocyanines: Synthesis, photophysical and nonlinear optical properties

Bolong Li<sup>a</sup>, Zengduo Cui<sup>a</sup>, Yuping Han<sup>b,\*\*</sup>, Jiale Ding<sup>a</sup>, Zhenhua Jiang<sup>a</sup>, Yunhe Zhang<sup>a,\*</sup>

<sup>a</sup> Engineering Research Center of Super Engineering Plastics, Ministry of Education, College of Chemistry, Jilin University, Changchun, 130012, PR China

<sup>b</sup> Department of Urology, China-Japan Union Hospital of Jilin University, Chang Chun, 130012, PR China

## ARTICLE INFO

### Keywords:

Phthalocyanine  
Anthraquinone  
Polyphenylsulfone  
Nonlinear optics  
Optical limiting  
Electron transfer

## ABSTRACT

Materials with excellent nonlinear optical (NLO) properties are usually applied in optoelectronics and optical limiting devices. Photoinduced intramolecular electron transfer (PET) and energy transfer (ET) play an important role in enhanced NLO properties. Through axially connected anthraquinone to phthalocyanine, two types of novel lanthanum phthalocyanine (LaPc-Aqn and HLaPc-Aqn) were designed to effectively improve PET/ET process, and thus leading to excellent NLO properties. Hyperbranched phthalocyanines possess enhanced NLO properties owing to their special three-dimensional structures that have more donor–acceptor (D–A) systems in their cell structure than lanthanum phthalocyanines. The uniform polyphenylsulfone composite film (HLaPc-Aqn-PPSU) was prepared by a simple solution casting method according to the “like dissolves like” theory. The values of large third-order nonlinear susceptibility ( $\text{Im}[\chi^{(3)}]$ ) and low limit threshold ( $I_{\text{lim}}$ ) were  $1.51 \times 10^{-9}$  esu and  $0.015 \text{ J/cm}^2$ , respectively, demonstrating that the film had great optical limiting performance. Such research can contribute to the development of novel phthalocyanine materials for nonlinear optics and optical limiting devices.

## 1. Introduction

Nonlinear optical (NLO) materials have attracted great attention due to their applications in photonics, telecommunication systems, data processing, and optical power limiting (OPL) [1–3]. Organic materials with fast response time and large optical nonlinearities have attracted growing attention, compared with a variety of other promising materials with outstanding NLO performance. Such organic materials effectively attenuate laser pulses to protect human eyes and optical components from exposure to intense light beams [4,5]. In recent years, metal phthalocyanines have been widely studied owing to their 18-electron conjugated macrocycle structure, photoelectric properties, and chemical and thermal stability. Meanwhile, several efforts have been made to successfully regulate the photophysical and NLO properties of phthalocyanine through metal coordination, substitutional effects and  $\pi$ -conjugate size [6–8].

The tuning of the NLO properties of phthalocyanines (Pcs) can be achieved by varying the centric atoms and placing substituents on the Pc ring. Previous studies have shown that Pcs could be coordinated with rare earth atoms such as lanthanum, holmium and ytterbium, helping

the intersystem crossing (ISC) between singlet states and triplet states through enhancing spin-orbit coupling [9]. Chen et al. synthesized a series of hyperbranched phthalocyanines with different substituents, and the Z-scan result indicated that NLO properties could be tailored further by placing substituents [7]. In addition, phthalocyanine-modified carbon-based nanomaterials have been extensively studied owing to their multiple optical limiting mechanisms [10,11]. Wang et al. synthesized a series of graphene hybrid materials that have been demonstrated to show a superior NLO response originating from the contribution of multiple optical limiting mechanisms [12]. Nevertheless, poor dispersion stability and machinability of the hybrid materials has restricted their prospective application in OPL devices. Moreover, it has been suggested that lanthanide double-decker phthalocyanines show modified NLO properties owing to their expanded  $\pi$  electron system and the presence of the heavy lanthanide central rare earth atom [13]. However, the extensive study and further application of double-decker phthalocyanines have been restricted because of the difficulty in preparation and low yield.

Another important representative of organic NLO materials, anthraquinone dye that possesses a highly delocalized  $\pi$ -electron system

\* Corresponding author.

\*\* Corresponding author

E-mail addresses: [blili17@mails.jlu.edu.cn](mailto:blili17@mails.jlu.edu.cn), [1545855940@qq.com](mailto:1545855940@qq.com) (Y. Han), [zhangyunhe@jlu.edu.cn](mailto:zhangyunhe@jlu.edu.cn) (Y. Zhang).

<https://doi.org/10.1016/j.dyepig.2020.108407>

Received 2 January 2020; Received in revised form 26 March 2020; Accepted 26 March 2020

Available online 4 April 2020

0143-7208/© 2020 Elsevier Ltd. All rights reserved.

in its nucleus [14]. As typical electron-acceptor, anthraquinones contain various types of chemical reaction sites that are widely used to modify material structures [15,16]. Pcs as a good electron donor can form a donor-acceptor (D-A) structure with anthraquinone through covalent connection. Fluorescence quenching and effective charge transfers in molecules caused by formation of D-A structure exert important significance for improving NLO properties [10,17].

For practical application, Pcs or other organic materials are often embedded in transparent polymers and the polymers could be used as substrates to turn materials into optical limiters [16]. Solid state optical limiters expand the use of materials and facilitate transportation. In addition, embedding the Pcs within a polymer thin film for OPL applications adds some protection to the Pcs against degradation [18]. Sakai Y et al. prepared polymer optics material through the covalent bonding of phthalocyanine and polymer [19]. However, the compounds exhibit low grafting ratio, which was a major obstacle to their application. Sekhosana K E et al. directly and physically mixed double-layer phthalocyanine materials into poly(methyl methacrylate) (PMMA) to prepare films, which presented excellent nonlinear properties and had a simple preparation process [13]. However, the phthalocyanines in the composite films prepared by this method cannot be uniformly dispersed, affecting the optical properties of the films.

In this work, two kinds of phthalocyanines, phenyl lanthanum phthalocyanine (compound 2) and hyperbranched lanthanum phthalocyanine (compound 5), were prepared. Next, lanthanum phthalocyanine derivatives (compounds 3 and 6) were obtained by axially connecting anthraquinone to compounds 2 and 5, respectively. Open aperture (OA) Z-scan technique was used to investigate the NLO performance of the samples. Because of the extended  $\pi$ -electron system and the formation of a D-A structure, the phthalocyanines axially bonded with anthraquinone, resulting in an effective Photoinduced intramolecular electron transfer (PET)/energy transfer (ET) process and excellent NLO performance. To facilitate practical application, compounds 5 and 6 were embedded in polyphenylsulfone (PPSU) films. The PPSU composite films possessed stronger NLO properties than solutions. As a kind of special engineering plastic, PPSU features good thermal stability, superior heat deflection temperature and flame resistance. Based on the principle of "like dissolves like", hyperbranched phthalocyanine and its derivatives can be well-dispersed with PPSU to form uniform and stable films.

## 2. Experimental section

### 2.1. Materials

4-Nitroptalonitrile, phenol, 4,4'-dihydroxydiphenylsulfone, 1-hydroxyanthraquinone, N, N-Dimethylformamide (DMF), lanthanum chloride hydrate (LaCl<sub>3</sub>), 1,8-diazabicyclo[5.4.0]undec-7-ene (DBU), n-pentanol, acetone, methanol and silver triflate were purchased from Aladdin Industry Company and used without further purification. PPSU was purchased from SOLVAY (model: RADEL R-5000) and used directly.

### 2.2. Instruments

IR spectra (KBr pellets) were recorded on a Nicolet iS10 FTIR spectrophotometer. The <sup>1</sup>H NMR spectra were recorded on a Bruker AVANCEIII600 instrument with dimethylsulfoxide-d<sub>6</sub> (DMSO-*d*<sub>6</sub>) as the solvent. Gel permeation chromatograms (GPC) employing polystyrene as a standard were obtained with an Agilent PL-GPC220 instrument with DMF as the eluent at a flow rate of 0.1 mL min<sup>-1</sup>. UV-vis absorption spectra were performed on UV2501-PC spectrophotometer. All MALDI-TOF-MS spectra were measured on a Bruker Autoflex speed TOF/TOF mass spectrometer. The nonlinear optical measurements were performed using an open aperture Z-scan technique employing a Q-switched Nd: YAG laser of 6 ns pulses at 532 nm with a repetition of 10 Hz. All liquid samples were placed in a 5 mm quartz cell and moved along the Z direction. Scanning electron microscopy (SEM) images were

obtained on a FEI Nova Nano 450 field mission SEM system and samples were aurum coated. X-ray photoelectron spectra was measured on PHI-1600 X-ray photoelectron spectrometer using Mg K $\alpha$  (1253.6 eV) radiation as the radiation source. Fluorescence spectra were recorded on a FLS 920 steady-transient spectrophotometer with a time-correlated single-photon counting system using a 400 nm laser source. The electrochemical data were obtained from Bio-Logic SP-150 electrochemical work station.

### 2.3. Synthesis

#### 2.3.1. Synthesis of 4-phenoxyphthalonitrile (1), Scheme 1

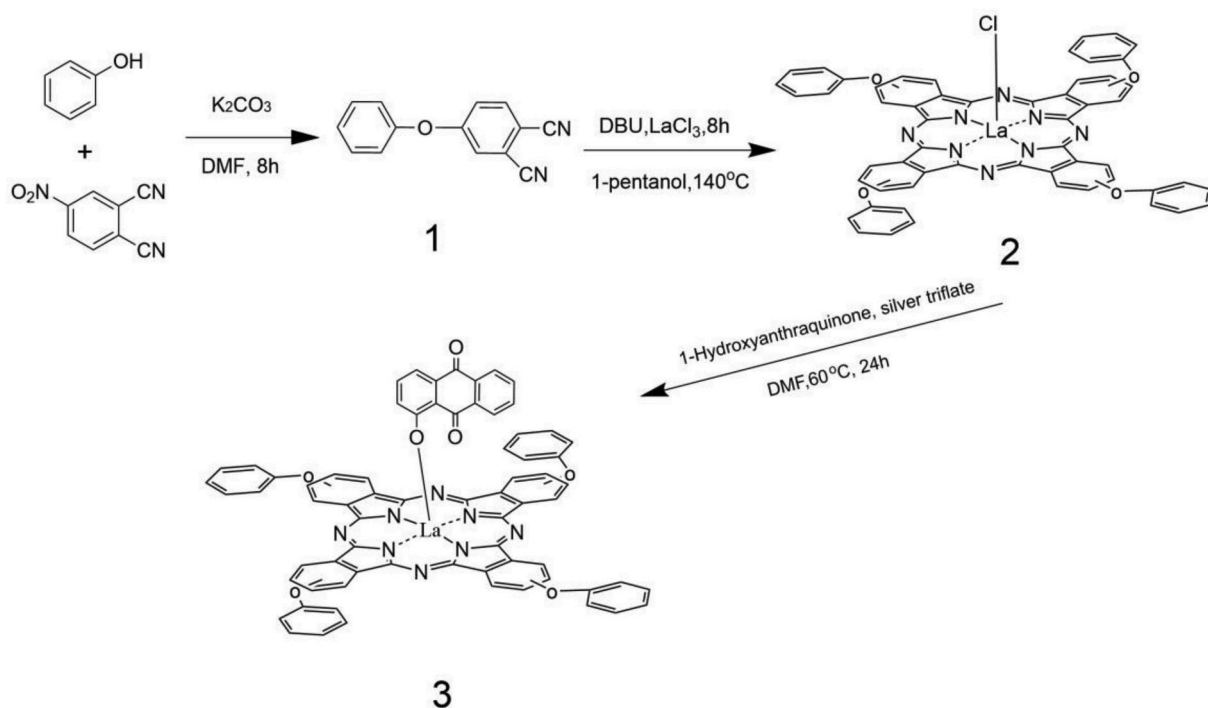
First, the solution of 4-nitroptalonitrile (3.46 g, 20 mmol) and phenol (1.88 g, 20 mmol) in 50 mL anhydrous N, N-Dimethylformamide (DMF) was stirred for 30 min under N<sub>2</sub>. Then, dry potassium carbonate (K<sub>2</sub>CO<sub>3</sub>) (5.52 g, 40 mmol) was added into above mixture products and stirred for 6 h at 80 °C. After cooling to room temperature, the mixture was poured into a large amount of deionized water. The reaction product was collected by filtration, and the solid was washed with deionized water until the filtrate became neutral, and crystallized by acetonitrile. Compound 1 was prepared according to previously reported methods [20]. Yield: 3.56 g (81%). FT-IR (KBr, cm<sup>-1</sup>): 2233, 1564, 1421, 1251, 1212, 1156, 1075, 872, 784, 694, 523. <sup>1</sup>H NMR (DMSO-*d*<sub>6</sub>)  $\delta$  8.12 (d, 1H), 7.81 (d, *J* = 2.6 Hz, 1H), 7.56–7.47 (m, 2H), 7.41–7.30 (m, 2H), 7.22 (dd, *J* = 9.9, 2.2 Hz, 2H) ppm. The detailed spectra of compound 1 are listed in the Supporting Information (Fig. S1 and Fig. S2).

#### 2.3.2. Synthesis of lanthanum(III) 2,9,16,23-tetrakis (4-phenoxy) phthalocyanine chlorine (2), Scheme 1

First, the solution of compound 1 (400 mg, 1.82 mmol) and LaCl<sub>3</sub> (147.2 mg, 0.6 mmol) in n-pentanol (30 mL) was stirred for 30 min under N<sub>2</sub>. Then, 0.5 mL of 1, 8-Diazabicyclo[5.4.0]undec-7-ene (DBU, 3.35 mmol) was added into above mixture products and was stirred for 8 h at 140 °C [9]. After cooling to room temperature, the product was precipitated out of solution by methanol. The reaction product was collected by filtration, and the solid was washed with methanol, deionized water in turn. Yield: 0.259 g (54%). FT-IR (KBr, cm<sup>-1</sup>): 1650, 1563, 1412, 1233, 1154, 1090, 1015, 944, 724. <sup>1</sup>H NMR (DMSO-*d*<sub>6</sub>)  $\delta$  7.99–7.65 (m, 5H), 7.64–7.54 (m, 4H), 7.53–7.31 (m, 10H), 7.31–7.04 (m, 10H), 7.03–6.87 (m, 3H) ppm. MALDI-TOF-MS (*m/z*): calcd for C<sub>56</sub>H<sub>32</sub>ClN<sub>8</sub>O<sub>4</sub>: 1054.13; found: 1054.2 (M<sup>+</sup>), 1019.3 (M<sup>+</sup>-Cl). elemental analysis calcd (%) for C<sub>56</sub>H<sub>32</sub>ClN<sub>8</sub>O<sub>4</sub>La: C 63.74, H 3.06, N 10.62; found: C 64.02, H 3.04, N 10.36. The detailed spectra of compound 2 are listed in the Supporting Information (Fig. S1 and Fig. S3).

#### 2.3.3. Synthesis of lanthanum(III) 2,9,16,23-tetrakis (4-phenoxy) phthalocyanine derivative (3), Scheme 1

First, the solution of compound 2 (211 mg, 0.2 mmol) and silver triflate (0.1 g) in anhydrous DMF (35 mL) was stirred for 12 h under N<sub>2</sub>. Then 1-hydroxyanthraquinone (67.2 mg, 0.3 mmol) in anhydrous DMF (15 mL) was added into above mixture products and stirred for 24 h at 60 °C under N<sub>2</sub>. The reaction mixture was poured into a large amount of deionized water. The product was collected by filtration and washed several times with acetone and deionized water to remove the excess reactants. Finally, the blue-green sample was obtained in the vacuum drying oven [19]. Yield: 0.192 g (74%). FT-IR (KBr, cm<sup>-1</sup>): 1650, 1629, 1585, 1473, 1419, 1227, 1156, 1074, 1010, 937, 879, 831, 723, 694, *m/z* = 1242. <sup>1</sup>H NMR (DMSO-*d*<sub>6</sub>)  $\delta$  8.21–8.28 (m, 2H), 7.99–7.65 (m, 9H), 7.64–7.54 (m, 4H), 7.53–7.38 (m, 11H), 7.31–7.04 (m, 10H), 7.03–6.88 (m, 3H) ppm. MALDI-TOF-MS (*m/z*): calcd for C<sub>70</sub>H<sub>39</sub>N<sub>8</sub>O<sub>7</sub>La: 1242.20; found: 1242.2 (M<sup>+</sup>). elemental analysis calcd (%) for C<sub>70</sub>H<sub>39</sub>N<sub>8</sub>O<sub>7</sub>La: C 67.64, H 3.16, N 9.01; found: C 67.39, H 3.18, N 8.76. The detailed spectra of compound 3 are listed in the Supporting Information (Fig. S1 and Fig. S4).



Scheme 1. Synthetic route of compounds 2 and 3.

#### 2.3.4. Synthesis of bis-[4-(3,4-dicyanophenoxy)phenyl]sulfone (4), Scheme 2

First, the solution of 4-nitrophthalonitrile (6.92 g, 40 mmol) and 4,4'-Sulfonyldiphenol (5.01 g, 20 mmol) in 50 mL anhydrous DMF was stirred for 30 min under  $N_2$ . Then, dry potassium carbonate ( $K_2CO_3$ ) (11.04 g, 80 mmol) was added into above mixture products and stirred for 6 h at 80 °C. After cooling to room temperature, the mixture was poured into a large amount of deionized water. The reaction product was collected by filtration, and the solid was washed with deionized water until the filtrate become neutral, and crystallized using acetonitrile. Compound 4 was prepared according to previously reported methods [21]. Yield: 8.14 g (81%). FT-IR (KBr,  $cm^{-1}$ ): 2236, 1578, 1484, 1313, 1250, 1151, 953, 682.  $^1H$  NMR (DMSO- $d_6$ )  $\delta$  8.18 (d,  $J = 8.7$  Hz, 1H), 8.07 (d,  $J = 8.8$  Hz, 2H), 8.02 (d,  $J = 2.5$  Hz, 1H), 7.62 (dd,  $J = 8.7, 2.6$  Hz, 1H), 7.37 (d,  $J = 8.8$  Hz, 2H) ppm. The detailed spectra of compound 4 is listed in the Supporting Information (Fig. S5 and Fig. S6).

#### 2.3.5. Synthesis of hyperbranched lanthanum (III) phthalocyanine (5), Scheme 2

First, the solution of compound 4 (2.259 g, 4.5 mmol) and anhydrous  $LaCl_3$  (557 mg, 1.5 mmol) in 40 mL anhydrous DMF and 7 mL n-pentanol were stirred for 30 min under  $N_2$ . Then, 0.5 ml of DBU (3.35 mmol) was added into above mixture and stirred for 8 h at 140 °C. After cooling to room temperature, the product was precipitated out of solution by methanol. The reaction product was collected by filtration, and the solid was washed with methanol, deionized water in turn [9]. The dark green solid was filtered and dried in vacuum, affording hyperbranched lanthanum phthalocyanine powder was recorded as compound 5. Yield: 1.64 g (71%). FT-IR (KBr,  $cm^{-1}$ ): 2234, 1580, 1481, 1299, 1230, 1105, 1099, 835, 724, 683.  $^1H$  NMR (DMSO- $d_6$ )  $\delta$  8.47–7.85 (m, 12H), 7.84–7.71 (m, 4H), 7.71–7.06 (m, 10H), 7.06–7.61 (m, 4H) ppm. GPC: Mn, 10100; Polydispersity, 1.13. The detailed spectra of compound 5 is listed in the Supporting Information (Fig. S5, Fig. S7 and Fig. S8).

#### 2.3.6. Synthesis of hyperbranched lanthanum (III) phthalocyanine derivative (6), Scheme 2

First, the solution of compound 5 (330 mg) and silver triflate (0.1 g) in anhydrous DMF (35 mL) was stirred for 12 h under  $N_2$ . Then 1-hydroxyanthraquinone (79 mg, 0.35 mmol) in anhydrous DMF (15 mL) was added into above mixture products and stirred for 24 h at 60 °C. The reaction mixture was poured into a large amount of deionized water. The product was collected by filtration and washed several times with acetone and deionized water to remove the excess reactants [19]. Finally, the dark green solid was filtered and dried in vacuum, affording hyperbranched lanthanum phthalocyanine powder was recorded as compound 6. Yield: 0.231 g (68%). FT-IR (KBr,  $cm^{-1}$ ): 2236, 1647, 1633, 1582, 1483, 1230, 1151, 1105, 835, 777, 724, 682.  $^1H$  NMR (DMSO- $d_6$ )  $\delta$  8.48–7.87 (m, 16H), 7.86–7.70 (m, 6H), 7.70–7.04 (m, 11H), 7.04–6.60 (m, 4H) ppm. GPC: Mn, 10600; Polydispersity, 1.20. The detailed spectra of compound 6 is listed in the Supporting Information (Fig. S5, Fig. S7 and Fig. S9).

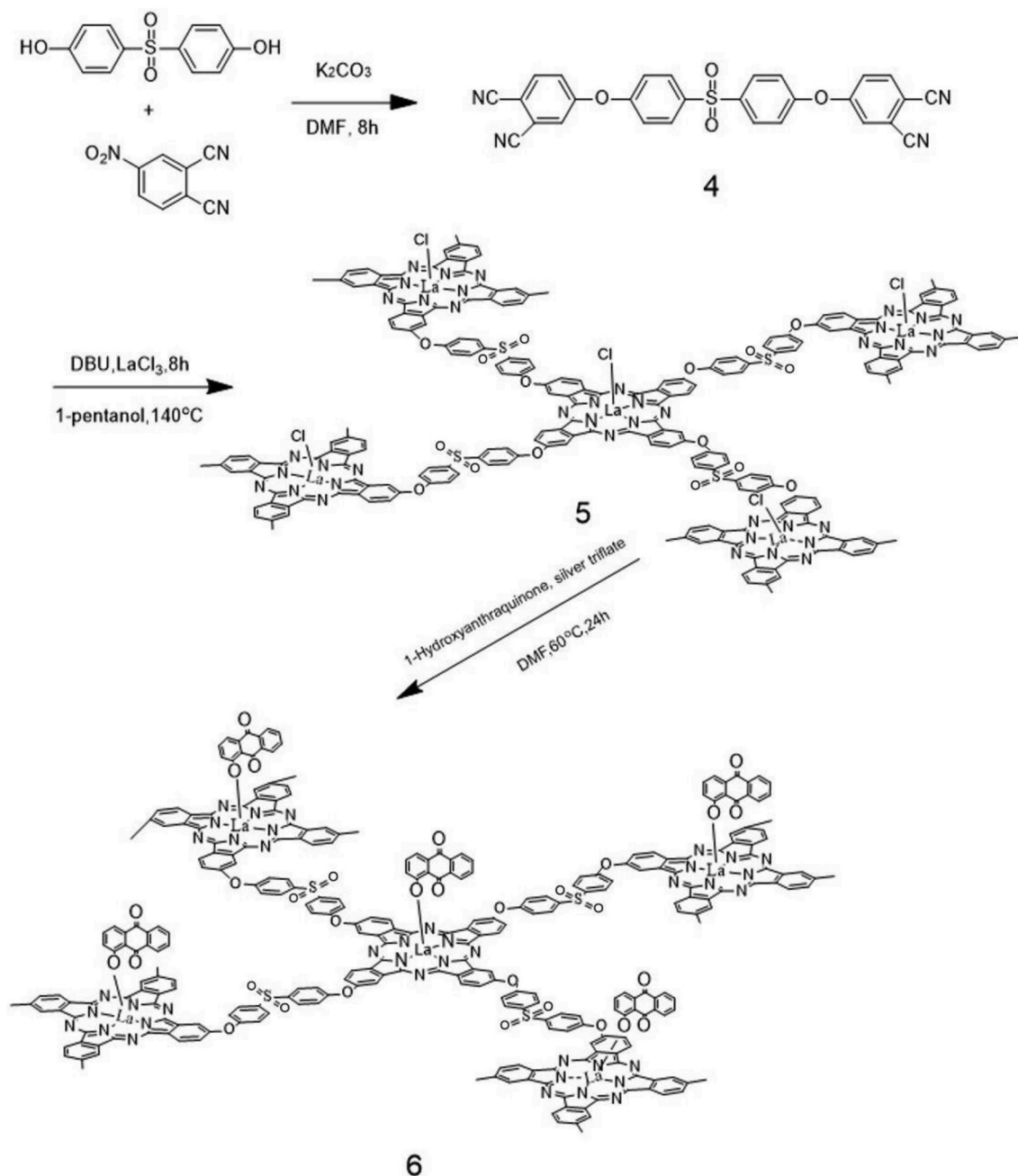
#### 2.4. Fabrication of composite films

Briefly, PPSU (0.3 g) and 6 mg of compounds 2, 3, 5, or 6 were, respectively, dissolved in NMP (12 mL) and stirred for 6 h until homogeneous mixtures of Pc-polymer solution were obtained. Drop the solution on the 8 × 8 cm glass plate, and then bake the glass plate containing the sample polymer solution in a vacuum oven at 80 °C for 8 h to completely evaporate NMP to obtain the film sample. A series of films with the thickness of 25  $\mu m$  were obtained. The prepared thin films are represented as 2-PPSU, 3-PPSU, 5-PPSU and 6-PPSU, respectively.

### 3. Results and discussions

#### 3.1. Synthesis and characterization

The procedure in Scheme 1 is a synthesis of 4-phenoxyphthalonitrile. Compound 2 was prepared by the condensation of 4-phenoxyphthalonitrile and anhydrous  $LaCl_3$ . 1-Hydroxyanthraquinone was attached to compound 2 through axial covalent bonding under the conditions



Scheme 2. Synthetic route of compounds 5 and 6.

catalyzed by silver triflate to synthesize compound 3. The process for the preparation of the compounds 5 and 6 are illustrated in the same method as shown in Scheme 2. Fig. 1 shows the  $^1H$  NMR spectra of 1-hydroxyanthraquinone (Aqn), 2 and 3. Compared with compound 2, we found that compound 3 exhibited the new bands at approximately 8.21–8.28 ppm and 7.99–7.65 ppm, which were attributed to the H of the anthraquinone groups. Meanwhile, the peak on the hydroxyl hydrogen atom of anthraquinone disappeared at 12.45 ppm, which proved the successful synthesis of compound 3.

The XPS spectra of compounds 2, 3, 5 and 6 are shown in Fig. 2. As shown in Fig. 2a, there were three peaks near 284 eV, 399 eV and 532 eV, corresponding to C 1s, N 1s and O 1s species, respectively [11]. The peak of La 4d was observed at 97.6 eV corresponding to the orbit d of La, and two peaks were observed at 836 eV and 853 eV, corresponding to  $3d_{5/2}$  and  $3d_{3/2}$  species, respectively, of La. However, compared with compounds 2 and 5, no peak related to Cl 2p, which is an element that

does not exist in the phthalocyanine derivatives, was observed in compounds 3 and 6; this indicates that Cl was substituted. Fig. 2b–e depicts the high-resolution XPS spectra of C 1s. The spectrum of C 1s can be fitted to four peaks, C-C at 284.5 eV, C-N at 285.8 eV, C=O at 288.2 eV and C-O at 288.4 eV, corresponding to different carbon species. For the spectra of compounds 2 and 5, a species corresponding to C=O was not found, while anthraquinone in compounds 3 and 6 corresponding to C=O species was found at 288.2 eV. The relevant FT-IR,  $^1H$  NMR, GPC and MALDI-TOF-MS spectra are shown in Fig. S1–S9. The image of the solution sample is shown in Fig. S10. All results mentioned above confirmed that compounds 2, 3, 5 and 6 were successfully synthesized.

### 3.2. Photophysical parameters

Fig. 3 shows the UV-Vis absorption spectra of the samples in the DMF solution. In UV-Vis spectra, all samples exhibited typical

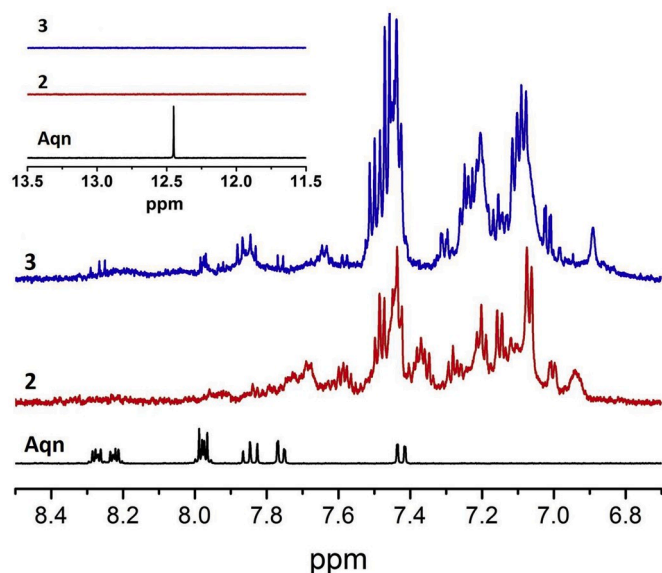


Fig. 1.  $^1\text{H}$  NMR spectra of 1-hydroxyanthraquinone (Aqn), compound 2 and compound 3.

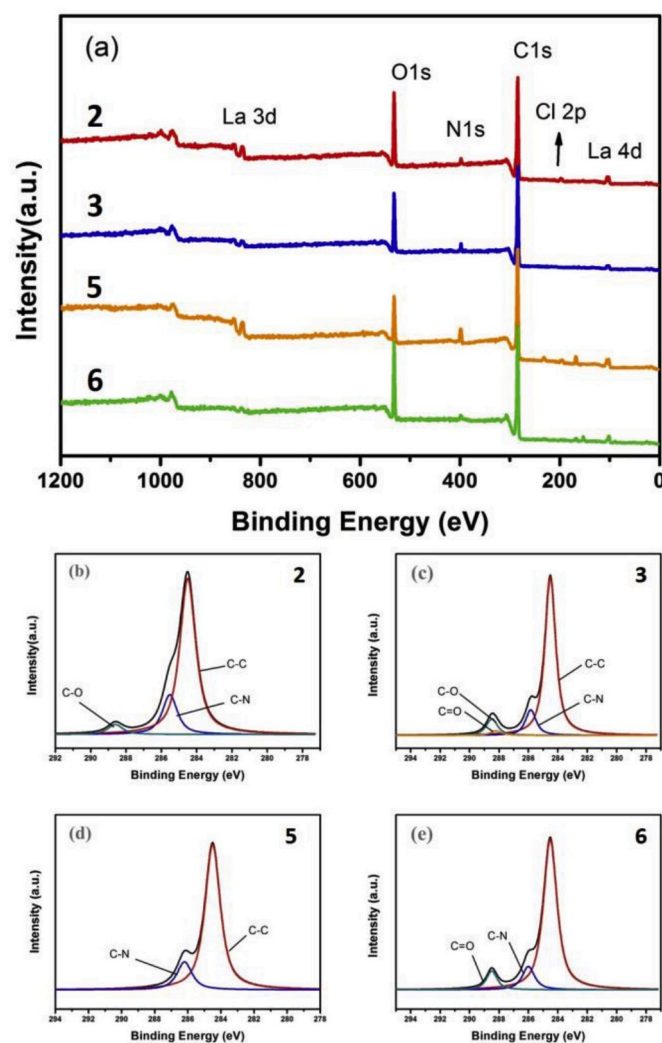


Fig. 2. XPS spectra of compounds 2, 3, 5 and 6.

phthalocyanine spectral behavior with two characteristic absorption peaks, one in the UV region of 300–400 nm (B band), another in the visible region of about 600–700 nm (Q band) due to the  $\pi\text{-}\pi^*$  transition [22,23]. Compound 2 had two narrow peaks in the Q band of the spectrum at 667 and 699 nm (Fig. 3a), owing to the oxygen in the phenoxy group in one phthalocyanine structure liable to be coordinated with  $\text{La}^{3+}$  of another phthalocyanine molecule to form Pc aggregates [24,25]. The structure of compound 3 increased the distance between the two molecules, which destroyed the structural features of the formation of aggregates. Reduced aggregation was known to positively affect photophysical parameters [26,27]. The absorption of compounds 5 and 6 are shown in Fig. 3b. Compound 5 had a hyperbranched structure with a highly branched three-dimensional molecular structure, which had difficulty in forming aggregates. Compound 6 showed B bands appearing in the region of 319–406 nm, and the Q band appeared in the region of 570–730 nm. These observations suggested the axial connection of the oxime group increased the conjugated system of the phthalocyanine, resulting in a change in its electronic state.

Given that the as-prepared phthalocyanine derivatives contained electron donor (Pc) and acceptor (Aqn) units, we studied the photo-induced intramolecular events by steady-state fluorescence spectra, and the results are shown in Fig. 4a. The efficient PET/ET played a crucial role in nonlinear optics [11,28]. At the excitation wavelength of 610 nm, the maximum emission peaks of compounds 2, 3, 5 and 6 correspond to approximately 706 nm, 709 nm, 689 nm and 696 nm, respectively. It was clear that fluorescence quenching had taken place in compounds 3 and 6 relative to that of compounds 2 and 5. This was due to the PET between the anthraquinone and the phthalocyanine ring, which meant the electron mobility of the entire phthalocyanine ring increased, and thus the molecule underwent fluorescence quenching [16,29]. The symmetry of the whole electron cloud was decreased after being axially connected, which facilitated the flow of the electron cloud. According to Fig. 4b and Table 1, the fluorescence lifetime ( $\tau_f$ ) and fluorescence quantum yield ( $\Phi_f$ ) of compound 3 was lower than those of compound 2. Compared with compound 3, the introduction of anthraquinone group in compound 6 has less effect on the fluorescence quantum yield, making the fluorescence quantum yield decreased slightly.

The energy level model was used to describe the interaction of light with the phthalocyanines in terms of PET/ET process (Fig.S11). There were several competing processes that could occur at different energy levels. However, another process usually happened from  $S_1$  state to charge separated state (CSS) by the PET when the D–A structure existed in the materials [11]. In addition, the fluorescence lifetime ( $\tau_f$ ) of compounds 3 and 6 were lower than those of compounds 2 and 5 (Table 1), respectively, suggesting that axially substituted phthalocyanines possessed a higher energy level of the  $S_1$  state than the unmodified lanthanum phthalocyanines. Therefore, the energy gap in axially substituted phthalocyanines between the  $S_1$  state and the  $T_1$  state was much lower than that of the unmodified lanthanum phthalocyanines, resulting in a higher value of the nonlinear absorption effect [30].

### 3.3. Nonlinear optical properties

To further study the OL performance of compounds 2, 3, 5 and 6 OA Z-scan measurements were performed. All the samples were dispersed in DMF at a concentration of 0.3 mg/mL. The Q-switched Nd:YAG laser provided a 4 ns laser pulse at 532 nm of second harmonic, with a repetition rate of 10 Hz and a pulse energy of 200  $\mu\text{J}$ . The transmitted beam of all samples along the Z position decreased, indicating that the sample exhibited positive nonlinear absorption, the shape of the Z-scan signal indicated that the samples had effective nonlinear optical parameters.

The normalized transmittances of compounds 2, 3, 5 and 6 at the focus (maximum input flux) were reduced to 0.93, 0.90, 0.87, and 0.79, respectively. When the sample moved to focus, compound 5 exhibited a

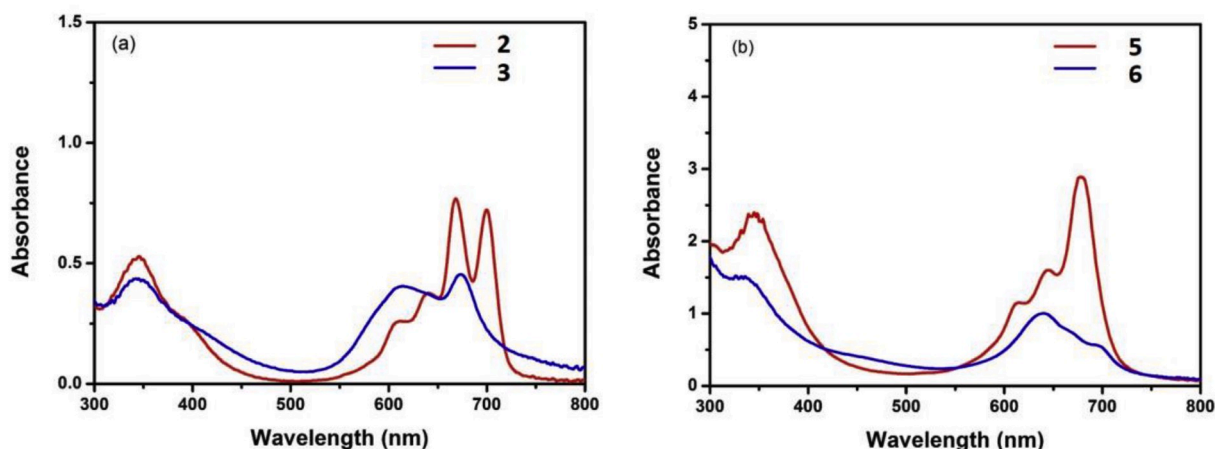


Fig. 3. UV-vis absorption spectra of compounds 2, 3, 5 and 6 in DMF at concentration  $2.5 \times 10^{-5}$  M.

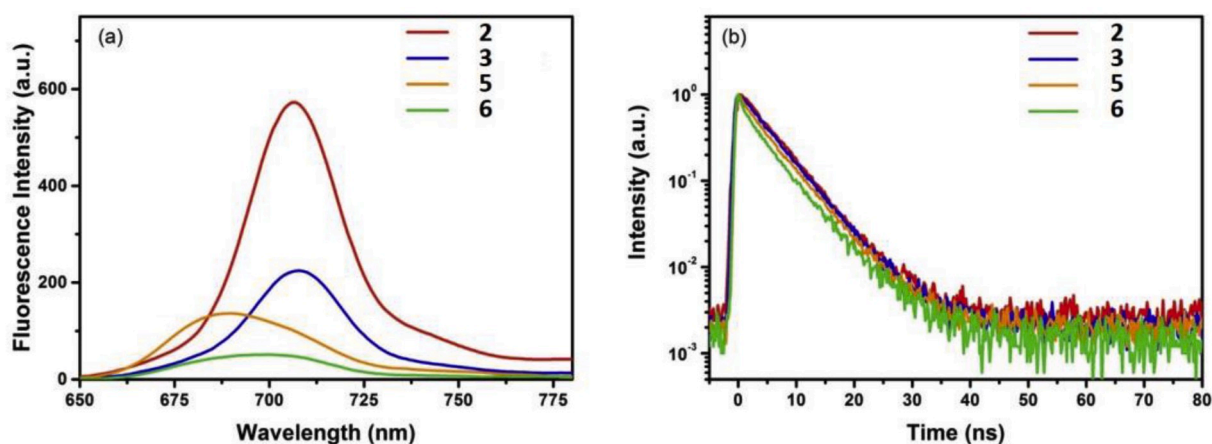


Fig. 4. Fluorescence spectra (a) and Fluorescence decay curves (b) of compounds 2, 3, 5 and 6 in DMF at concentration  $2.5 \times 10^{-5}$  M.

Table 1

Fluorescence properties and nonlinear optical parameters of compounds 2, 3, 5 and 6 in DMF.

|  | 2                      | 3                      | 5                      | 6                      |
|--|------------------------|------------------------|------------------------|------------------------|
| $\lambda_{\max}$ (nm)                        | 706                    | 709                    | 689                    | 696                    |
| $\Phi_F$                                     | 0.17                   | 0.11                   | 0.06                   | 0.05                   |
| $\tau_F$ (ns)                                | 5.32                   | 5.26                   | 5.11                   | 4.87                   |
| $I_0$ ( $\mu\text{J}$ )                      | 200                    | 200                    | 200                    | 200                    |
| LT (%)                                       | 80                     | 80                     | 84                     | 76                     |
| $\alpha_0$ ( $\text{cm}^{-1}$ )              | 0.43                   | 0.44                   | 0.34                   | 0.55                   |
| $\beta_{\text{eff}}$ ( $\text{cm GW}^{-1}$ ) | 0.43                   | 0.51                   | 0.60                   | 1.52                   |
| $\text{Im}[\chi^{(3)}]$ (esu)                | $1.41 \times 10^{-13}$ | $1.67 \times 10^{-13}$ | $1.97 \times 10^{-13}$ | $4.99 \times 10^{-13}$ |

more prominent two-photon absorption (TPA) processes than compound 2. Furthermore, the nonlinear absorption coefficients of two axially-connected phthalocyanines were larger than phthalocyanines in Fig. 5. It was clear that the compounds 3 and 6 exhibit much better NLO performances than compounds 2 and 5, which meant that the introduction of the anthraquinone enhanced the NLO response of phthalocyanines. The corresponding parameters were obtained by fitting the numerical data, and the results are shown in Table 1. The nonlinear absorption coefficient  $\beta_{\text{eff}}$  ( $\text{cm GW}^{-1}$ ) could be calculated as equation (1) through the experimental data:

$$T_{OA} = \sum_{m=0}^{\infty} \frac{[-\beta_{\text{eff}} I_0 L_{\text{eff}} / (1 + (z/z_0)^2)]^m}{(m+1)^{3/2}} \quad (1)$$

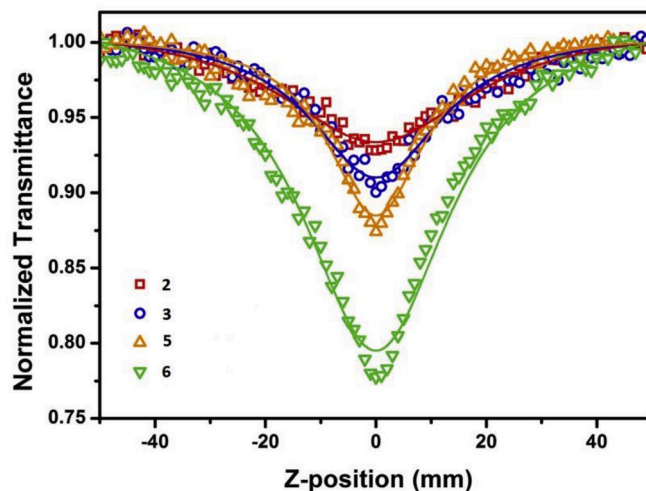


Fig. 5. Open-aperture Z-scan curves of compounds 2, 3, 5 and 6 in DMF at 532 nm.

$T_{OA}$  refers to the measured hole transmittance, and  $L_{\text{eff}}$  is the effective thickness of the sample.  $L_{\text{eff}} = [1 - \exp(-\alpha L)]/\alpha$ ,  $\alpha$  is the linear absorption rate of the sample.  $I_0$  is the axial light intensity of the samples and  $z$  is the position of the sample.  $z_0$  ( $z_0 = \pi \omega_0^2/\lambda$ ) is the Rayleigh range, where  $\omega_0$  is the beam waist at focal point ( $z = 0$ ) and  $\lambda$  is the wavelength

of incident light [31,32].

The third-order nonlinear susceptibility  $\text{Im}[\chi^{(3)}]$  is a parameter of the firmness of a molecular material against perturbation caused by a laser pulse, and is expressed in terms of  $\beta_{\text{eff}}$  using equation (2) [33]:

$$\text{Im}[\chi^{(3)}] = n_0^2 \varepsilon_0 c \lambda \beta_{\text{eff}} / 2\pi \quad (2)$$

where  $n_0$  is the linear refractive index,  $c$  is the speed of light in vacuum, and  $\varepsilon_0$  is the permittivity of a vacuum. According to the definition of  $\text{Im}[\chi^{(3)}]$ , the change rule of  $\text{Im}[\chi^{(3)}]$  under the same measurement conditions is consistent with that of  $\beta_{\text{eff}}$  [34]. Therefore, the larger the value of  $\text{Im}[\chi^{(3)}]$ , the better the nonlinear optical absorption performance of the material.

As manifested in Table 1, compound 6 shows superior NLO properties to other samples, and its  $\beta_{\text{eff}}$  reached  $1.52 \text{ cm GW}^{-1}$ , which was 2.5 times higher than that of compound 5. In particular, the  $\beta_{\text{eff}}$  of compound 3 was 1.2 times larger than that of compound 2. Compounds 3 and 6 exhibited a modified NLO performance in comparison with that of compounds 2 and 5, which further proved the existence of a cumulative effect due to the axial bonding between anthraquinone and Pcs. The  $\text{Im}[\chi^{(3)}]$  of compounds 2, 3, 5 and 6 reached  $1.41 \times 10^{-13}$  esu,  $1.67 \times 10^{-13}$  esu,  $1.97 \times 10^{-13}$  esu and  $4.99 \times 10^{-13}$  esu, respectively (Table 1). The anthraquinone in compounds 3 and 6 could reduce the symmetry of the electron cloud system and facilitate its flow [35]. It is clear that  $\beta_{\text{eff}}$  of compound 6 was higher than that of compound 3 for the following reasons. The introduction of the anthraquinone group as the electron acceptor can form D–A structure with every phthalocyanine ring in compound 6, thus compound 6 has several D–A systems in a cell structure, which promotes the effective PET/ET process. Furthermore, the anthraquinone axial connection of phthalocyanines could increase the electron cloud density and show obvious fluorescence decay, which would be beneficial for the electron transfer process. It has been verified by fluorescence spectra and fluorescence quantum yield data.

### 3.4. Electrochemical properties

In order to gain insight into the effect on the NLO properties due to axially connecting anthraquinone to phthalocyanine, the molecular orbital energy levels of phthalocyanine and anthraquinone were obtained and compared. According to the cyclic voltammetry spectra (Fig. S12) and UV–vis spectrum (Fig. 3), the lowest unoccupied molecular orbital level of compounds 2 and 3 were obtained by using equation (3) [36].

$$E_{\text{LUMO}}(\text{eV}) = -e(4.8 - E_{\text{FC}} + E_{\text{OX}}) + E_{\text{g}} \quad (3)$$

where  $E_{\text{g}}$  is the HOMO–LUMO gap of Pc;  $E_{\text{g}} = hc/\lambda = 1240/\lambda$ ,  $\lambda$  being the absorption edge (Table S1);  $E_{\text{ox}}$  is the onset of oxidation potential of Pc;  $E_{\text{FC}} = (E_{\text{ox}} + E_{\text{red}})/2 = 0.5$  is the energy level of ferrocene used as a standard, and the LUMO levels of the anthraquinone as obtained by  $E_{\text{LUMO}}(\text{eV}) = -e(4.8 - E_{\text{FC}} + E_{\text{red}})$  [37],  $E_{\text{red}}$  being the onset of reduction potential of anthraquinone.

It is found that the LUMO energy level of anthraquinone ( $E_{\text{LUMO}} = -3.68 \text{ eV}$ ) was lower than that of compounds 2 and 5 as shown in Table 2. The electrons in the LUMO of phthalocyanine could easily transit to the low-energy LUMO of anthraquinone and led to the

**Table 2**

$E_{\text{g}}$ , LUMO Energy Levels, and  $\Delta E$  data of the samples.

|     | $E_{\text{g}}(\text{eV})$ | $E_{\text{LUMO}}(\text{eV})$ | $\Delta E(\text{eV})^a$ |
|-----|---------------------------|------------------------------|-------------------------|
| 2   | 1.701                     | −3.13                        | −                       |
| 3   | 1.736                     | −                            | 0.550                   |
| 5   | 1.715                     | −3.10                        | −                       |
| 6   | 1.714                     | −                            | 0.587                   |
| Aqn | 2.672                     | −3.68                        | −                       |

<sup>a</sup>  $\Delta E = E_{\text{LUMO}}(\text{Pc}) - E_{\text{LUMO}}(\text{Aqn})$ .

expanded flow range of electrons, resulting in the improvement of NLO properties of phthalocyanines [38]. Compared with compound 3 (0.550), compound 6 (0.587) had a larger discrepancy  $\Delta E$  between the LUMO level of phthalocyanine and anthraquinone. Thus, large LUMO levels of phthalocyanines were thought to be the important factors for the enhanced NLO effect. The LUMO energy level further confirmed that ET can occur between phthalocyanine moieties acting as electron donor and anthraquinone moiety acting as the electron acceptor [39].

### 3.5. Optical limiting properties of composite films

From a practical application point of view, an effective way to get optical limiting devices that can be easily transported and stored is to realize the transformation of NLO properties of materials from organic compound solutions to solid films. Previous studies have noted that the phthalocyanines embedded in polymer as films have better optical limiting performance than phthalocyanine solution [40]. The uniform dispersion of phthalocyanine in polymer films is important for stable performance of optical limiting properties. The hyperbranched phthalocyanines can be uniformly dispersed in the composite film, and the reduction of the aggregate can ensure that the material effectively plays the optical limiting effect. When laser irradiated, the uniform composite films ensure that each part of the film has the same nonlinear optical response. In addition, reducing the aggregation also helps to improve the PET/ET process of phthalocyanine and further enhance nonlinear optical performance. The optical microscopy images of composite films are shown in Fig. 6. For the sake of observation, the composite films were placed on the paper with text. Clearly, compounds 2 and 3 had aggregation tendencies in thin films. Compounds 5 and 6 were well-dispersed in PPSU films, and no obvious inhomogeneity was observed. Hyperbranched phthalocyanines and PPSU both had sulfone groups in their structures. The highly similar structures made for excellent uniform films. Based on the “like dissolves like” theory, compounds 5, and 6 significantly improved their homogeneity and dispersion stability in the polymer-based materials.

To further observe the micro-morphology of the films, Fig. 7 and Fig. S13 display the SEM images of 2-PPSU, 3-PPSU, 5-PPSU and 6-PPSU. Apparently, there was a significant dispersion difference wherein a certain amount of compound 2 deposition occurred in 2-PPSU, and a significant amount of agglomerated particles were deposited on one side of the 2-PPSU (Fig. 7a). The deposition of 3-PPSU was also obvious (Fig. 7b). In contrast, 5-PPSU and 6-PPSU were dispersed evenly in the films (Fig. 7c and d), and no obvious precipitation area was observed due to the distinct of hyperbranched structure. The hyperbranched phthalocyanine and its derivatives had a sulfone group structure, the PPSU polymer also had this structure, which allowed compounds 5 and 6 to be well-dispersed in the PPSU films and to show good optical properties.

The nonlinear optical properties of 5-PPSU and 6-PPSU were studied under the same conditions as the solution using Z-scan (Fig. 8a). We place the films sample vertically and clamp them on the mold vertically, and the mold moves uniformly along the Z axis direction. A significant decrease in the transmittance of composite films at the focal can be observed. The linear transmission values of 64% and 59% were respectively measured for 5-PPSU and 6-PPSU. The NLO properties of composite films were immensely improved and the  $\beta_{\text{eff}}$  of 5-PPSU and 6-PPSU could reach  $2678.29 \text{ cm GW}^{-1}$  and  $3542.58 \text{ cm GW}^{-1}$ , respectively. The considerable enhancement of NLO performance was derived from the stabilization of the polymer and the conjugated electrons of a large number of benzene rings in the PPSU. In addition, 6-PPSU has the superior NLO performance of compound 6 and uniform dispersion in PPSU. The OA Z-scan of polymer-based films showed that the introduction of the anthraquinone structure gave the material a greater normalized transmittance valley depth, indicating that the enhanced NLO properties stemmed from the intracomplex PET/ET process [38].

Incident intensity threshold ( $I_{\text{lim}}$ ) is defined as the input strength

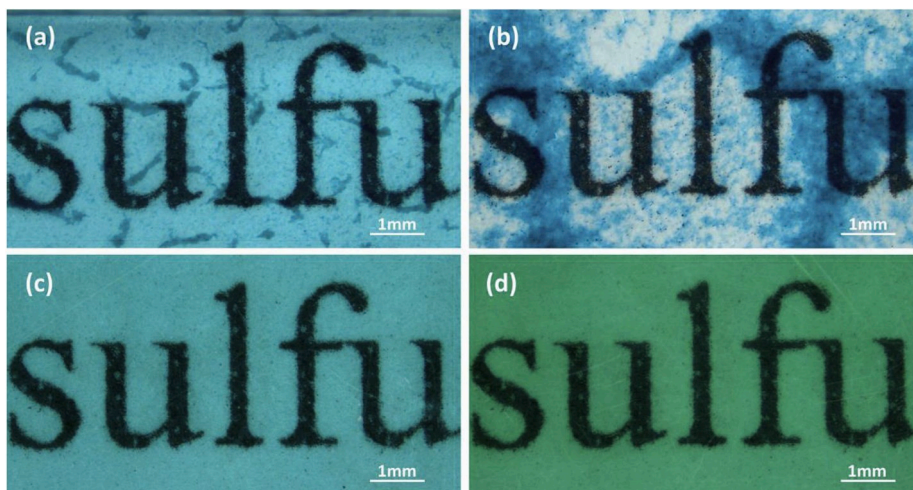


Fig. 6. Optical microscope images of 2-PPSU (a), 3-PPSU (b), 5-PPSU (c), and 6-PPSU (d).

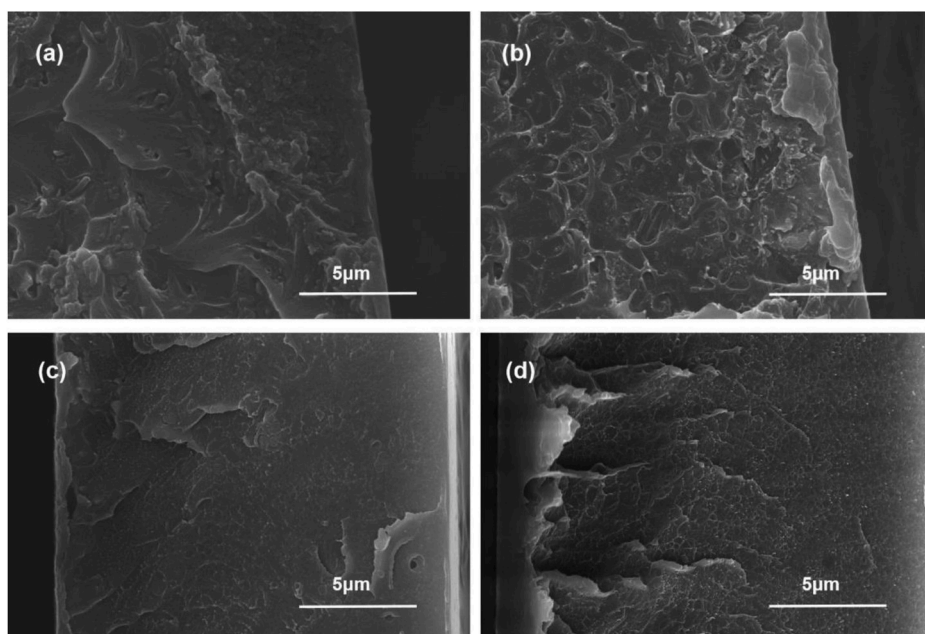


Fig. 7. SEM images of 2-PPSU (a), 3-PPSU (b), 5-PPSU (c) and 6-PPSU (d).

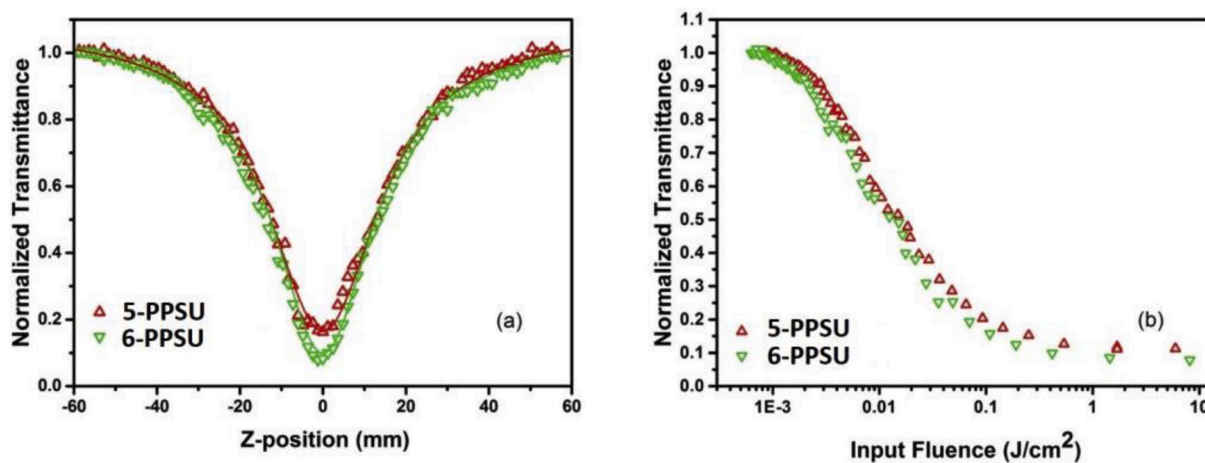


Fig. 8. Open-aperture Z-scan curves(a) and Optical limiting plots of normalized transmittance versus incident fluence (b) for PPSU films at 532 nm.

when the linear transmittance of the material is 0.5 (50%). Therefore, the low  $I_{lim}$  signified that the material played a role in optical limitation field and has broad prospective applications. The optical limiting curve of the composite material in PPSU thin films is given by plotting the energy density versus normalized transmittance (Fig. 8b). At low energy density, the transmittance remained almost constant and did not change with incident energy density, following Lambert-Beer's law. At high energy density (above  $\sim 0.002 \text{ J/cm}^2$ ), the transmittance decreased as the energy density of the incident light increased and deviated from linearity. The  $I_{lim}$  value of **5-PPSU** and **6-PPSU** were  $0.019 \text{ J/cm}^2$  and  $0.015 \text{ J/cm}^2$ , respectively, which showed excellent optical limiting performance. **6-PPSU** demonstrated superior optical limiting properties, originating from a synergy between the polymer and phthalocyanine and the excellent nonlinear optical properties of compound **6** itself.

#### 4. Conclusion

In this study, we have designed two novel lanthanum phthalocyanine derivatives modified with anthraquinone through axial substitution. The fluorescence quenching, short fluorescence lifetime, low fluorescence quantum yield, and discrepancy of LUMO levels have proved that novel axially substituted lanthanum phthalocyanines have an effective PET/ET process. Owing to the accumulation effect of the D–A system, highly branched structure, and the PET/ET process, hyperbranched lanthanum phthalocyanine derivative not only exhibited NLO properties superior to those of unmodified hyperbranch phthalocyanine, but also outperformed lanthanum phthalocyanine derivative. In addition, the composite films prepared by solution casting exhibited remarkable uniformity owing to the “like dissolves like” theory. The PPSU-based composite films possessed excellent NLO properties and optical limiting effects. Our results suggest that these phthalocyanines and their composite films show strong NLO properties and optical limiting performance that can make them suitable candidates for optical limiting devices.

#### Declaration of competing interest

The authors declare no conflict of interest.

#### CRediT authorship contribution statement

**Bolong Li:** Writing - original draft, Conceptualization, Formal analysis. **Zengduo Cui:** Data curation, Writing - original draft. **Yuping Han:** Data curation. **Jiale Ding:** Validation. **Zhenhua Jiang:** Resources. **Yunhe Zhang:** Writing - review & editing, Conceptualization, Supervision.

#### Acknowledgements

This work was financially supported by National Natural Science Foundation of China (No. 51973080 and 51573070) and Jilin Province Science and Technology Development Plan Project (20190302051GX).

#### Appendix A. Supplementary data

Supplementary data to this article can be found online at <https://doi.org/10.1016/j.dyepig.2020.108407>.

#### References

- Bonaccorso Z F, Sun T H, Ferrari AC. Graphene photonics and optoelectronics. *Nat Photon* 2010;4:611–22.
- Dudley JM, Taylor JR. Ten years of nonlinear optics in photonic crystal fibre. *Nat Photon* 2009;3(2):85–90.
- Wang T, Wang X, Zhang J, Wang C, Shao J, Jiang Z, Zhang Y. Synthesis, structure and third-order optical nonlinearities of hyperbranched metal phthalocyanines containing imide units. *Dyes Pigments* 2018;154:75–81.
- Aijian W, Laixiang C, Xiaodong C, et al. Reduced graphene oxide covalently functionalized with polyaniline for efficient optical nonlinearities at 532 and 1064 nm. *Dyes Pigments* 2018;160:344–52.
- Xu Y, Wang W, Ge Y, Guo H, Zhang X, Chen S, Zhang H. Stabilization of black phosphorous quantum dots in PMMA nanofiber film and broadband nonlinear optics and ultrafast photonics application. *Adv Funct Mater* 2017;27(32):1702437.
- Kabwe KP, Louzada M, Britton J, Olomola TO, Nyokong T, Khene S. Nonlinear optical properties of metal free and nickel binuclear phthalocyanines. *Dyes Pigments* 2019;168:347–56.
- Chen X, Zhang J, Wei WW, et al. Synthesis and third-order optical nonlinearities of hyperbranched metal phthalocyanines. *Eur Polym J* 2014;53:58–64.
- Xiao Z, Li Z, Wu X, et al. Ultrafast excited-state dynamics of Ni-contained covalently bonded phthalocyanine-porphyrin conjugates. *Dyes Pigments* 2015;127:197–203.
- Zhao P, Wang Z, Chen J, Zhou Y, Zhang F. Nonlinear optical and optical limiting properties of polymeric carboxyl phthalocyanine coordinated with rare earth atom. *Opt Mater* 2017;66:98–105.
- Wang A, Ye J, Humphrey MG, et al. Graphene and carbon-nanotube nanohybrids covalently functionalized by porphyrins and phthalocyanines for optoelectronic properties. *Adv Mater* 2018;30(17):1705704.
- Zhao C, He C, Dong Y, Song W. The third order nonlinear optical properties of graphene oxide-zinc (II) naphthalocyanine hybrids and amino graphene oxide-zinc (II) naphthalocyanine hybrids. *Carbon* 2019;145:640–9.
- Wang X, Ding J, Dong N, Jiang Z, Zhang Y, Wang J. Covalent functionalization of graphene oxide with hyperbranched lanthanum phthalocyanines for improving optical limiting. *Mater Lett* 2020;258:126781.
- Sekhosana KE, Nyokong T. The nonlinear absorption in new lanthanide double decker pyridine-based phthalocyanines in solution and thin films. *Opt Mater* 2015;47:211–8.
- Jeyaram S, Geethakrishnan T. Low power laser induced NLO properties and optical limiting of an anthraquinone dye using Z-scan technique. *J Mater Sci Mater Electron* 2017;28(13):9820–7.
- Nian-Youa C, Sheng-Fang Z, Guo-An C. Microwave synthesis of a novel porphyrin-anthraquinone and its photoinduced electron transfer properties. *Chem Reag* 2013;35(1):24–6.
- Tao M, Liu L, Liu D, et al. Photoinduced energy and electron transfer in porphyrin-anthraquinone dyads bridged with a triazine group. *Dyes Pigments* 2010;85(1–2):21–6.
- Wang A, Zhao W, Chen X, et al. Coordination-induced broadband optical nonlinearity through axial bonding of pyridine anchored methine-bridged polypyrrrole to metal-porphyrins. *Dyes Pigments* 2018;157:20–6.
- Kumar GA. Optical studies of phthalocyanine molecules in PMMA matrix. *Mater Lett* 2002;55(6):364–9.
- Sakai Y, Ueda M, Yahagi A, et al. Synthesis and properties of aluminum phthalocyanine side-chain polyimide for third-order nonlinear optics. *Polymer* 2002;43(12):3497–503.
- Yuta N, Nobuhiro T, Kenta Y, Jun M, Teruaki H, Masa-aki K. Syntheses of carboxylated poly(arylene ether ketone)s with hyperbranched and linear architectures through the self-condensations of aromatic dicarboxylic anhydrides. *Polym J* 2018;50(12):1149–57.
- Peng X, Sheng H, Guo H, Kimiyoshi N, Yu X, Ding H, Qu X, Zhang Q. Synthesis and properties of a novel high-temperature diphenyl sulfone-based phthalonitrile polymer. *High Perform Polym* 2014;26(7):837–45.
- Arslanoglu Y, Mertsev M, Hamuryudan E, Gul A. Near-IR absorbing phthalocyanines. *Dyes Pigments* 2006;68(2–3):129–32.
- Nas A, Kahriman N, Kantekin H, et al. The synthesis of novel unmetallated and metallated phthalocyanines including (E)-4-(3-cinnamoylphenoxy) groups at the peripheral positions and photophysical properties of their zinc phthalocyanine derivatives. *Dyes Pigments* 2013;99(1):90–8.
- Zhang XF, Xi Q, Zhao J. Fluorescent and triplet state photoactive J-type phthalocyanine nano assemblies: controlled formation and photosensitizing properties. *J Mater Chem* 2010;20(32):6726.
- Kameyama K, Morisue M, Satake A, et al. Highly fluorescent self-coordinated phthalocyanine dimers. *Angew.Chemie* 2005;117(30):4841–4.
- Bian YH, Chen JS, Xu ST, Zhou YL, Zhu LJ, Xiang YZ, Xia DH. The effect of a hydrogen bond on the supramolecular self-aggregation mode and the extent of metal-free benzoxazole-substituted phthalocyanines. *New J Chem* 2015;39:5750–8.
- Shirk JS, Pong RGS, Flom SR, Heckmann H, Hanack M. Effect of axial substitution on the optical limiting properties of indium phthalocyanines. *J Phys Chem A* 2000;538:1438–49. 104.
- Torre GDL, Vázquez Purificación, Agulló-López F, et al. Role of structural factors in the nonlinear optical properties of phthalocyanines and related compounds. *Chem Rev* 2004;104(9):3723–50.
- Qiumei G, Limin C, Sujian P, et al. Morpholinyl dendrimer phthalocyanine: synthesis, photophysical properties and photoinduced intramolecular electron transfer. *Dalton Trans* 2018;10:1039.
- Chen J Xu Y, Cao M, et al. Strong reverse saturable absorption effect of a nonaggregated phthalocyanine-grafted MA-VA polymer. *J Mater Chem C* 2018;6:9767–77.
- Wu DS, Cheng WD, Li XD, Lan YZ, Chen DG, Zhang YC, Zhang H, Gong Y. ChemInform abstract: syntheses, crystal and electronic structures, and linear optics of LiMBO<sub>3</sub> (M: Sr, Ba) orthoborates. *J Phys Chem A* 2004;108:1837–43.
- Nalwa HS, Hanack M, Pawlowski G, Engel MK. Third-order nonlinear optical properties of porphyrazine, phthalocyanine and naphthalocyanine germanium

- derivatives: demonstrating the effect of  $\pi$ -conjugation length on third-order optical nonlinearity of two-dimensional molecules. *Chem Phys* 1999;245:17–26.
- [33] Sheik-Bahae M, Said AA, Wei TH, Hagan DJ, Van Stryland EW. Sensitive measurement of optical nonlinearities using a single beam. *IEEE J Quant Electron* 1990;26:760–9.
- [34] Garcia-Frutos EM, O'Flaherty SM, Maya EM, et al. Alkynyl substituted phthalocyanine derivatives as targets for optical limiting. *J Mater Chem* 2003;13(4):749–53.
- [35] Hanack M, Schneider T, Barthel M, et al. Indium phthalocyanines and naphthalocyanines for optical limiting. *Coord Chem Rev* 2001;219(3):235–58.
- [36] Shehzad FK, Zhou Y, Zhang L, et al. Anionic effect of  $\delta$  and  $\chi$  forms of tris(alkoxo) ligand functionalized anderson-type polyoxometalates on nonlinear optical response of porphyrin–POM based supramolecular compounds. *J Phys Chem C* 2018;122(2):1280–7.
- [37] Geskin VM, Lambert C, Brédas JL. Origin of high second and third-order nonlinear optical response in ammonio/borato diphenylpolyene zwitterions: the remarkable role of polarized aromatic groups. *J Am Chem Soc* 2003;125:15651–8.
- [38] Augur A, Blau WJ, Burnhamk PM, Chambrier I, Cook MJ, Isare B, Nekelsona F, O'Flaherty M. Nonlinear absorption properties of some 1,4,8,11,15,18,22, 25-octaalkylphthalocyanines and their metallated derivatives. *J Mater Chem* 2003;13:1042–7.
- [39] Zhu G, Long Y, Ren H, et al. Notable third-order optical nonlinearities realized in layer-by-layer assembled composite films by intercalation of porphyrin/polyoxometalate into layered double hydroxide. *J Phys Chem C* 2016;120(39):22549–57.
- [40] Bankole OM, Nyokong T. Mercaptopyrindine-substituted indium, zinc, and metal-free phthalocyanines: nonlinear optical studies in solution and on polymer matrices. *J Coord Chem* 2015;68(20):3727–40.